Supplementary information

X-ray Structure of the Carboplatin-loaded Apo-Ferritin nanocage

Nicola Pontillo,[a] Giarita Ferraro,[a] John R. Helliwell,[b] Angela Amoresano,[a] and Antonello Merlino[a,c*]

[a]*Department of Chemical Sciences, University of Naples Federico II, Complesso Universitario di Monte Sant'Angelo, Via Cintia, I-80126, Napoli, Italy. Fax: +39081674090; Tel: +39081674276; E-mail: antonello.merlino@unina.it*
[b]*School of Chemistry, Faculty of Engineering and Physical Sciences, University of Manchester, Brunswick Street, Manchester M13 9PL, England*
[c]*CNR Institute of Biostructures and Bioimages, Via Mezzocannone 16, I-80126, Napoli, Italy*

Methods

Sample preparation and preliminary characterization

Horse spleen ferritin (Ft) and carboplatin (CBDCA) were purchased from Sigma and used without further purification. CBDCA solutions were freshly prepared before each encapsulation experiment. A stock solution of Ft (90% L-chain, code F4503) was stored at 4 °C in 0.15 mM sodium chloride. The CBDCA-encapsulated AFt was prepared following the procedure that was used to obtain CDDP-encapsulated AFt [1]. In particular, protein (20 mg x mL^{-1}) was dissociated at pH 13 in the presence of CBDCA (protein subunit to metal drug ratios range from 1:30 to 1:280) and then reassembled at neutral pH. 0.1 M NaOH was used to slowly reach pH 13. After 30 min, the pH of the resulting solution was lowered to 7.0 using 1.0 M sodium phosphate buffer. After this process, the sample was dialyzed against 10 mM sodium phosphate buffer, pH 7 and ultra-filtered (with a 5 kDa cutoff) to remove precipitates and excess of the drug. Protein folding upon drug encapsulation was evaluated by collecting Far-UV CD spectra on a Jasco spectropolarimeter with a Peltier thermocontrol element (Jasco), in the range of λ=190–250 nm, using a protein concentration of 0.1 mg x mL^{-1} in 10 mM sodium phosphate pH 7.0.

Inductively coupled plasma mass spectrometry (ICP-MS) measurements were used to verify CBDCA encapsulation. These data indicate that CBDCA-encapsulated AFt contained Pt in a variable amount, depending on the preparation. The protein nanocage can encapsulate between 25 and 144 Pt atoms. In our hands, encapsulation experiments produced ferritin samples with an undetectable amount of iron. The Pt concentration in the protein samples was measured by ICP-MS using the following procedure: protein samples were suspended in 600 µl 65 % HNO_3 and 200 µl 35% HCl overnight at 90 °C. The acid solution was transferred into polystyrene liners, diluted 1:10 v/v with 5% HNO_3 and finally analyzed with an Agilent 7700 ICP-MS from Agilent Technologies, equipped with a frequency-matching RF generator and 3rd generation Octopole Reaction System (ORS3), operating with helium gas in ORF. Multi-element calibration standards were prepared in 5% HNO_3 at 4 different concentrations (1, 10, 50, and 100 µg x L^{-1}). All the analyses were performed as triplicates.

Crystallization, X-ray diffraction data collections, structure solution and refinement

Crystals of CBDCA-encapsulated AFt were obtained using a sample containing Pt in a 1:6 Ft subunit to metal ratio. Crystals were grown at 298 K in a week using the hanging-drop vapor diffusion method, when mixing equal volumes of protein (5 mg x mL-1) and reservoir solution. The crystallization conditions were 0.8 M $(NH_4)_2SO_4$, 0.1 M Tris-HCl pH 7.7, 60 mM $CdSO_4$. Diffraction data were first collected at 100 K at the CNR Institute of Biostructures and Bioimages in Napoli using a CuKα wavelength. Crystals were flash cooled in liquid N_2 after a 10 s soak in a cryoprotectant solution containing the reservoir and 20-25% glycerol. Intensity integration and scaling was performed using HKL2000 [2]. Data were then recollected later using a different crystal, but grown under the same conditions, at 100 K at the ID30a beamline of ESRF synchrotron, using λ=0.9677 Å; albeit a not tunable beamline it provided the necessary elemental discrimination that we sought. Reduction and scaling of these diffraction data were performed using iMosflm and POINTLESS/SCALA [3]. The statistics of the two data sets are reported in Table S1.

The structure of the CBDCA-encapsulated AFt was solved by the difference Fourier method, using the PDB file 5ERK without waters and ligands as a starting model [1]. The model was refined with Refmac5.8 [4] from the CCP4 suite [5]. Electron density map visualization and manual adjustments of the model were performed using Coot [6]. The structure of CBDCA-encapsulated AFt solved using data collected at ESRF refined to a Rfactor of 0.158 (Rfree 0.181); the structure solved using diffraction data collected at CNR Institute of Biostructures and Bioimages in Napoli refined to a Rfactor of 0.146 (Rfree 0.192).

Model refinement statistics are reported in Table S1. Structure validations were carried out using Procheck [7]. Coordinates and structure factors of the CBDCA-encapsulated AFt have been deposited in the Protein Data Bank under accession codes 5MIJ and 5MIK. Validation reports were available for the review process. The figures displayed in this paper were prepared using PyMOL [8].

Discrimination between Cd^{2+} and Pt^{2+}

It should be recalled that in this structure the Pt assignment is not straightforward, since Cd^{2+} ions are present in the crystallization conditions and thus many Cd^{2+} ions are bound to the protein surface. The position of Pt atoms is distinguished from those of Cd^{2+} ions by comparing the anomalous difference electron density map peaks at the two X-ray wavelengths. The f'' of Cd and of the Pt signals change in opposite ways, when data collected with CuKα are compared to those collected at an X-ray wavelength of 0.9677 Å: the Pt signal increases from about 7 electrons to 9 electrons and the Cd signal drops from 4.7 electrons to 2 electrons. Thus, the comparison of the anomalous difference Fourier electron density map peaks at the two X-ray wavelengths elegantly reveals which peaks should be attributed to Pt and which ones to Cd. Additional confirmations of the assignments were obtained by comparing 2Fo-Fc electron density maps of CBDCA-encapsulated AFt with those of the control (see Figure S2). Analyses of these maps clearly reveal that Pt is bound to His49. Indeed, in this binding site, a residual electron density is observed, close to one of the two conformations of His49. Furthermore, close to the other conformation of the His49, a large electron density peak, not observed in the control, is evident. Additional evidence is also obtained for the His132 binding site. Here, the electron

density map of CBDCA-encapsulated AFt is not so dissimilar to that of the control, but there is an additional peak close to Asp127, which we have attributed to a Cd ion that was displaced from its initial position close to the His132 side chain.

Comparison with the structure of CDDP-encapsulated AFt

First we compared the structures of CDDP-encapsulated AFt (PDB code 5ERJ) and CBD-encapsulated AFt (PDB code 5MIJ) by analyzing the root mean square deviations between their Cα atoms (RMSD). RMSD is as low as 0.52 Å. This finding indicates that there are no significant differences in the overall structure of the protein in the two complexes. Then we analyzed RMSD per residue. Data indicate that major differences (> 1 Å) are located at residue 1, and at residues 146-149, whereas more limited differences (> 0.3 Å) are located at residues 136-140 and 143-145, i.e. within the helix constituted by residues133-158. These results are confirmed by inspection of a difference distance matrix plot [9] generated using ddmp (Center for Structural Biology, Yale University, New Haven, CT, USA), which indicates modest conformational changes in the comparison between the two structures.

Finally, we analyzed the variations at the Pt binding sites: significant differences are found in the two structures. In CDDP-encapsulated AFt, Pt binds to the ND1 atom of His132, whereas in the case of CBDCA-encapsulated AFt, Pt binds to the NE2 atom of His132 and to the NE2 atom of His49, with the side chain of this residue adopting two different conformations and a Pt atom that also interacts with side chains of Glu45. In CDDP-encapsulated AFt, the NE2 atom of His132 binds a Cd^{2+} ion; His49 adopts two different conformations, with the two side chain conformers that form a hydrogen bond with a water molecule or is bound to a Cd^{2+} ion, which in turn interacts also with the side chain of Glu45.

References

[1] Pontillo, N.; Pane, F.; Messori, L.; Amoresano, A.; Merlino, A. Cis-platin encapsulation within a ferritin nanocage: a high-resolution crystallographic study. *Chem. Commun*. (Camb) **2016**, 52, 4136-4139.

[2] Otwinowski, Z.; Minor, W. Processing X-ray diffraction data collected in oscillation mode. *Methods Enzymol*.,**1997**, 276, 307-326.

[3] Battye, T.G.G.; Kontogiannis, L.; Johnson, O.; Powell, H.R.; Leslie, A.G.W. iMOSFLM: a new graphical interface for diffraction-image processing with MOSFLM. *Acta Crystallogr., Sect. D: Biol. Crystallogr*,. **2011**, 67, 271-281.

[4] Murshudov, G. N.; Skubak, P.; Lebedev, A. A.; Pannu, N. S.; Steiner, R. A.; Nicholls, R. A.; Winn, M. D.; Long, F.; Vagin, A. A. REFMAC 5 for the refinement of macromolecular crystal structures. *Acta Crystallogr., Sect. D: Biol. Crystallogr.*, **2011**, 67, 355-367.

[5] Winn, M. D. et al. Overview of the CCP4 suite and current developments. *Acta Cryst. D Biol Crystallogr* **2011**, 67, 235–242.

[6] Emsley, P.; Lohkamp, B.; Scott, W. G.; Cowtan, K. Features and development of Coot. *Acta Crystallogr D Biol Crystallogr*. **2010**, 66, 486–501.

[7] Laskowski, R. A.; Macarthur, M. W.; Moss, D. S.; Thornton, J. M. PROCHECK: A program to check the stereochemical quality of protein structures. *J. Appl. Cryst*., **1993**, 26, 283-291.

[8] W. L. DeLano, 2002. *PyMOL*. http://www.pymol.org .

[9] Richards, F.M.; Kundrot, C.E.. Identification of structural motifs from protein coordinate data: secondary structure and first-level supersecondary structure. *Proteins*. **1988**, 3,71–84

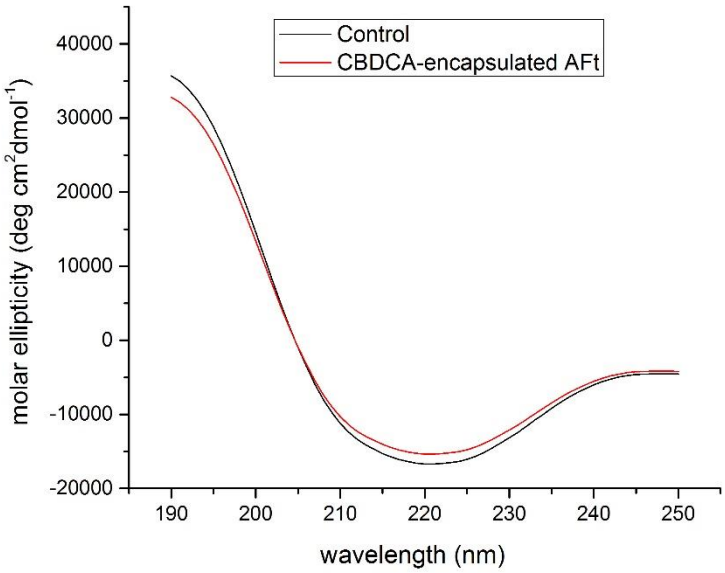

Figure S1. Far UV-CD spectra of CBDCA-encapsulated AFt and of the control at 0.1 mg x mL^{-1} in 10 mM sodium phosphate pH 7.0.

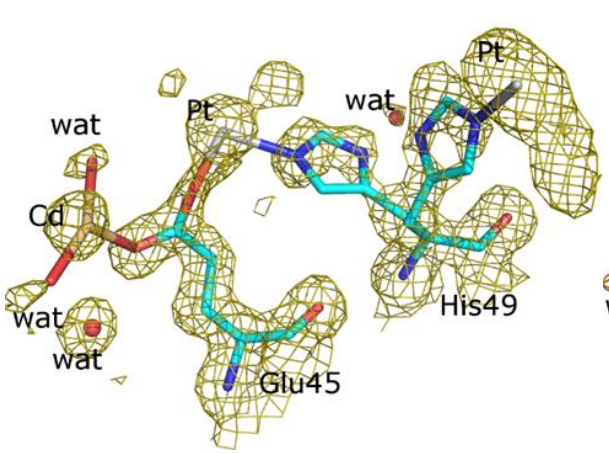
Pt
wat
Pt
wat
Cd
wat
wat
Glu45
His49

A

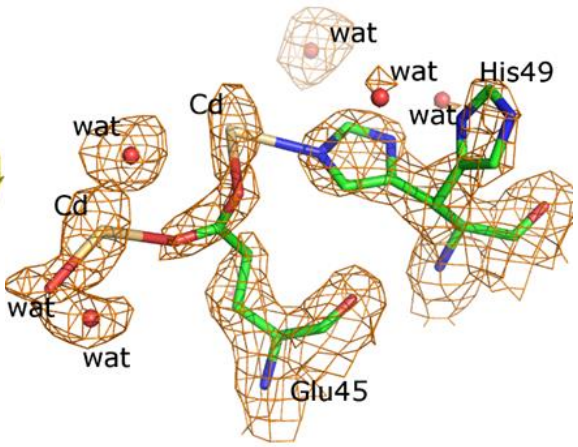
wat
wat
His49
Cd
wat
wat
Cd
wat
wat
Glu45

B

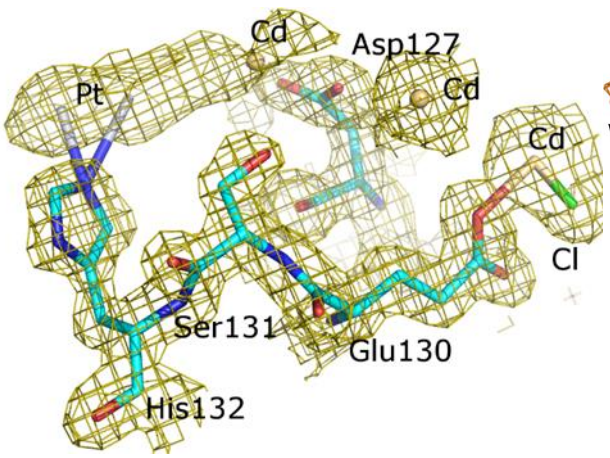
Cd
Asp127
Pt
Cd
Cd
Cl
Ser131
Glu130
His132

C

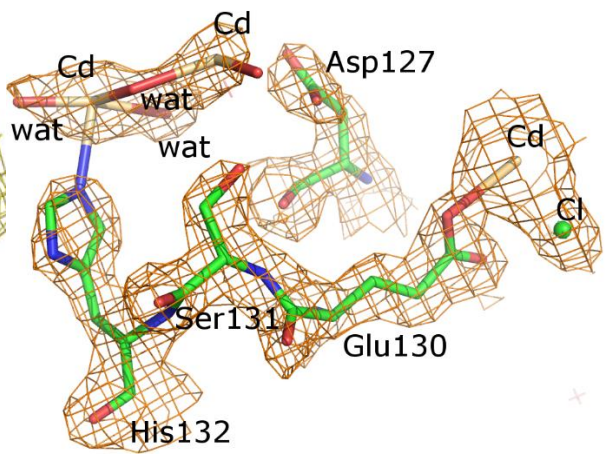
Cd
Cd
Asp127
wat
wat
wat
Cd
Cl
Ser131
Glu130
His132

D

Figure S2. Comparison of 2Fo-Fc electron density maps of Pt binding sites in CBDCA-encapsulated AFt (panels A and C) and of the electron density maps of the same regions in the control (panels B and D). Electron density maps are contoured at 1.0 and 3.0 σ, in olive and orange, for CBDCA-encapsulated AFt and control, respectively.

Table S1. Data collection and refinement statistics

	CBDCA-encapsulated AFt	CBDCA-encapsulated AFt
Data Collection statistics X-ray source	ESRF synchrotron	Rotating anode
Wavelength	λ=0.9677Å	λ=1.5418Å
Space group	F432	F432
Unit-cell parameters a=b= c (Å), α,β,γ (°)	 181.67 90	 180.65 90
Ft Monomers per a. u.	1	1
Resolution (Å)	104.9-1.49 (1.52-1.49)	104.3-1.96 (2.00-1.96)
Observed reflections	371229	129618
Unique reflections	42236	18700
Completeness (%)	99.7 (99.1)	99.9 (100)
Rmerge	0.084 (0.429)	0.107 (0.489)
Rpim	0.030 (0.150)	0.040 (0.209)
I/σ(I)	14.8 (4.2)	6.2 (3.8)
Multiplicity	8.6 (9.0)	6.9 (5.2)
Refinement		
Resolution (Å)	104.9-1.49	104.3-1.96
n. of reflections in working set	39899	17792
n. of reflections in test set	2123	904
R factor/Rfree (%)	15.8/18.1	14.6/19.2
n of non-H atoms in the refinement	1782	1725
Occupancy of Pt ions	0.30, 0.30, 0.30, 0.30	0.30, 0.30, 0.30, 0.30
B-factor of Pt ions (Å^2)	43.4, 42.0, 46.0, 25.4	71.3, 94.3, 63.9, 46.9
Overall B-factor	15.7	20.8
Deviations from ideality values R.m.s.d. bonds (Å)	0.032	0.018
R.m.s.d. angles (Å)	2.18	1.73